Pergamon

Geochimica et Cosmochimica Acta, Vol. 67, No. 15, pp. 2725–2733, 2003

0016-7037/03 $30.00 + .00

doi:10.1016/S0016-7037(03)00108-X

Rates of oxygen exchange between the $Al_2O_8Al_{28}(OH)_{56}(H_2O)_{26}^{18+}$(aq) ($Al_{30}$) molecule and aqueous solution

BRIAN L. PHILLIPS,[2] ALASDAIR LEE,[1] and WILLIAM H. CASEY[1,3,*]

[1]Department of Land Air and Water Resources, University of California, Davis, CA 95616-8627 USA
[2]Department of Geosciences, State University of New York, Stony Brook, NY 11794-2100 USA
[3]Department of Geology, University of California, Davis, CA 95616-8627 USA

(*Received October* 8, 2002; *accepted in revised form January* 10, 2003)

Abstract—Rates of steady exchange of oxygens between bulk solution and the largest known aluminum polyoxocation: $Al_2O_8Al_{28}(OH)_{56}(H_2O)_{26}^{18+}$(aq) ($Al_{30}$) are reported at pH≈4.7 and 32–40°C. The Al_{30} molecule is a useful model for geochemists because it is ≈2 nm in length, comparable to the smallest colloidal solids, and it has structural complexity greater than the surfaces of most aluminum (hydr)oxide minerals. The Al_{30} molecule has 15 distinct hydroxyl sites and eight symmetrically distinct bound waters. Among the hydroxyl bridges are two sets of μ_3-OH, which are not present in any of the other aluminum polyoxocations that have yet been studied by NMR methods. Rates of isotopic equilibration of the μ_2-OH and μ_3-OH hydroxyls and bound water molecules fall within the same range as we have determined for other aluminum solutes, although it is impossible to determine rate laws for exchange at the large number of individual oxygen sites. After injection of ^{17}O-enriched water, growth of the ^{17}O-NMR peak near 37 ppm, which is assigned to μ_2-OH and μ_3-OH hydroxyl bridges, indicates that these bridges equilibrate within two weeks at temperatures near 35°C. The peak at +22 ppm in the ^{17}O-NMR spectra, assigned to bound water molecules (η-OH_2), varies in width with temperature in a similar fashion as for other aluminum solutes, suggesting that most of the η-OH_2 sites exchange with bulk solution at rates that fall within the range observed for other aluminum complexes. Signal from one anomalous group of four η-OH_2 sites is not observed, indicating that these sites exchange at least a factor of ten more rapidly than the other η-OH_2 sites on the Al_{30}. *Copyright © 2003 Elsevier Ltd*

1. INTRODUCTION

Earth scientists will come to rely heavily on computer simulations of geochemical reactions because so many environments are either in geologic settings that are impossible to sample or because the time scales are too large for experiment. Methods of computational chemistry are advancing rapidly but they simulate molecular-scale processes, not bulk reactions. There is relatively little information on geochemically important molecular-scale reactions, yet understanding these processes is essential for improving our computer methods.

To advance this field, we are determining rates of oxygen exchange at different sites in simple aluminum molecules using NMR spectroscopy. The molecules range in size from simple aqueous monomers (e.g., AlF^{2+}; Yu et al., 2001) to multimeric complexes that are intermediate in size between a monomeric solute and a colloidal solid (Phillips et al., 2000; Casey et al., 2000; Casey and Phillips, 2001; Lee et al., 2002).

Multimeric species are particularly important because they expose distinct sets of bridging oxygens to the aqueous solution, which our studies show can have surprisingly different reactivities. For example, there are two types of bridging hydroxyls in the MAl_{12} ε-Keggin complexes (MAl_{12} = Al_{13}, $GaAl_{12}$, $GeAl_{12}$) that differ principally in their position relative to the μ_4-O. For any one of these molecules, these two sets of μ_2-OH exchange oxygens with bulk solution at rates that differ by a factor of at least 44. Substitutions at metal sites several bonds away from the μ_2-OH also dramatically affect the rates of oxygen-isotope exchange (Phillips et al., 2000; Casey et al., 2000; Casey and Phillips, 2001; Lee et al., 2002), yet the rates of exchange of bound water molecules with the bulk vary only by a factor of about five and fall into the same range as aluminum monomers. Furthermore, for the Al_{13} molecule, the bridging hydroxyls exchange many times before a molecule dissolves and dissolution appears to be controlled by reactions at highly coordinated interior oxygens (i.e., μ_4-O). Similar behavior might be expected for minerals, such as boehmite, that expose μ_4-O and μ_2-OH, particularly if they are exposed at the edges of crystallites and steps.

In the present work, we extend our work to the largest aluminum polyoxocation for which the structure is known, the Al_{30} (Al_{30} = $Al_2O_8Al_{28}(OH)_{56}(H_2O)_{26}^{18+}$(aq)) molecule. The Al_{30} is ≈2 nm in length and exposes oxygens in many different coordination environments to the aqueous solution. Although the polymer was first identified in ^{27}Al-NMR spectra several years ago (Fu et al., 1991), it was only recently crystallized by Allouche et al. (2000) and Rowsell and Nazar (2000) for X-ray determination of the structure and stoichiometry.

1.1. Structure of the Al_{30} Molecule

The structure of the Al_{30} is best understood by first examining the smaller ε- and δ-Keggin isomers of the Al_{13} molecules (Figure 1) because they are building blocks for the larger Al_{30}. The Al_{13} molecule that is most familiar to geochemists is the ε-isomer of the Keggin family of structures (see Pope 1983, p. 27). The Al_{13} version of the ε-MAl_{12} molecules has been

* Author to whom correspondence should be addressed (whcasey@ucdavis.edu).

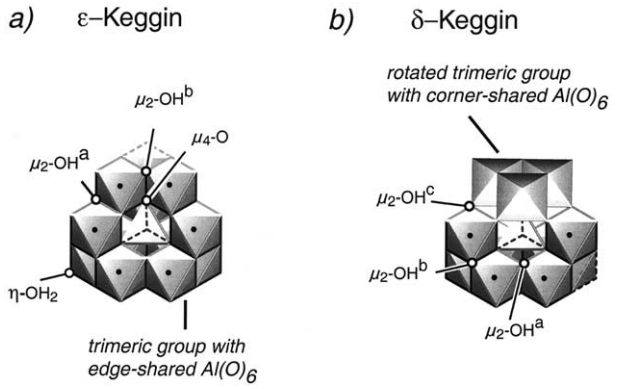

Fig. 1. Polyhedral representation of two known isomers of the Al_{13} polyoxocations: **a)** The ε-Keggin isomer has four distinct types of oxygens (see Phillips et al., 2000). There are twelve identical bound water molecules (η-OH_2), four identical μ_4-O and two sets of twelve μ_2-OH (labeled μ_2-OH^a and μ_2-OH^b) that are distinguished by their position relative to the μ_4-O. **b)** The δ-Keggin Al_{13} molecule is similar to the ε-Keggin, but has one trimeric group rotated 60° so that it links to other trimeric groups by corner-shared $Al(O)_6$, not edge-shared $Al(O)_6$ as in the ε-Keggin isomer. The rotated cap gives rise to an additional topologically distinct μ_2-OH (labeled μ_2-OH^c) that links two corner-shared $Al(O)_6$ and reduces the symmetry to C_{3v}, producing additional symmetrically distinct sites for μ_2-OH^a and μ_2-OH^b.

found in nature (Hunter and Ross, 1991; Rao and Rao, 1992) and has long been used as an experimental model for mineral surfaces (e.g., Wehrli et al., 1990; Bradley et al., 1993; Phillips et al., 2000). The ε-Al_{13} exhibits T_d symmetry and contains four types of oxygens (Fig. 1-a.): (i) bound water molecules (η-OH_2; multiplicity twelve), (ii, iii) two structurally distinct hydroxyl bridges (μ_2-OH^a; μ_2-OH^b; twelve each), and (iv) four-coordinated oxo groups (μ_4-O; multiplicity four). The structure can be viewed as consisting of four (Al_3O_{13}) trimeric groups, each containing the μ_2-OH^b-μ_4-O edges. These trimers are connected to one another through the μ_2-OH^a-μ_2-OH^a edges (Fig. 1-a).

The δ-isomer of the Al_{13} molecule differs from the ε-isomer by rotation of one of the four (Al_3O_{13}) trimeric groups by 60° so that it links to the rest of the molecule through six shared apices, not edges (Fig. 1-b). The δ-Al_{13} structure has more types of oxygens than the ε-Al_{13} molecule because of the introduction of the corner-shared μ_2-OH^c and the resulting reduction in symmetry from T_d to C_{3v}. For example, the δ-Al_{13} contains three distinct sets of η-OH_2 and two types of μ_4-O, based upon their positions relative to the rotated trimer (see Fig. 1-b).

The Al_{30} molecule can be viewed as two δ-Al_{13} molecules that face one another at the rotated trimers and are bonded via two distinct $Al(O)_6$ linkages (Fig. 2.)

1. ***Linkage Set #1*** consists of $Al(O)_6$ groups that share three edges at the apices of the δ-Al_{13} units, forming a nonplanar tetrameric cap on each of the two δ-Al_{13}-like molecules. These linkages form three adjacent μ_3-OH groups on each tetrameric subunit.
2. ***Linkage Set #2*** consists of $Al(O)_6$ groups that connect the two modified δ-Keggin molecules to one another at the tetramer caps, via four corner-shared μ_2-OH bridges.

Although there are 15 inequivalent hydroxyls in the Al_{30}, assuming C_{2h} symmetry, it is useful to identify a smaller number of topologically distinct groups (Fig. 3, Table 1) that contain sites of similar structural positions, but are symmetrically inequivalent:

1. Eighteen μ_2-OH linking edges of $Al(O)_6$ together within the unrotated Al_3O_{13} trimers. These μ_2-OH(1) sites are analogous to μ_2-OH^b of the ε-Keggin Al_{13} (Fig. 1) and lie adjacent to one μ_4-O.
2. Twelve μ_2-OH linking the edges of (Al_3O_{13}) trimers together in the δ-Al_{13}-like subunits. These μ_2-OH(2) sites are analogous to the μ_2-OH^a in Figure 1 and are adjacent to two μ_4-O.
3. Twelve corner-linking μ_2-OH(3) formed by rotation of one of the (Al_3O_{13}) trimers in the two δ-Al_{13}-like moieties.

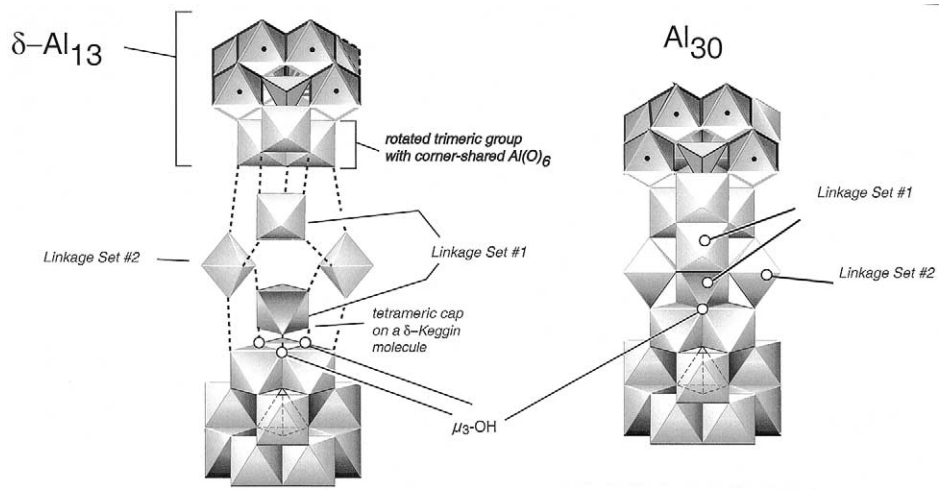

Fig. 2. The Al_{30} structure viewed with the two δ-Keggin Al_{13} moieties separated (left) and two sets of connecting $Al(O)_6$ polyhedra identified as Linkage Set #1 and Linkage Set #2. The same molecule in unexploded view is on the right. Solid symbols (●) are placed on the edge-shared (Al_3O_{13}) trimeric groups to emphasize the similarity of this structure with the ε-Keggin isomer (Figure 1-a).

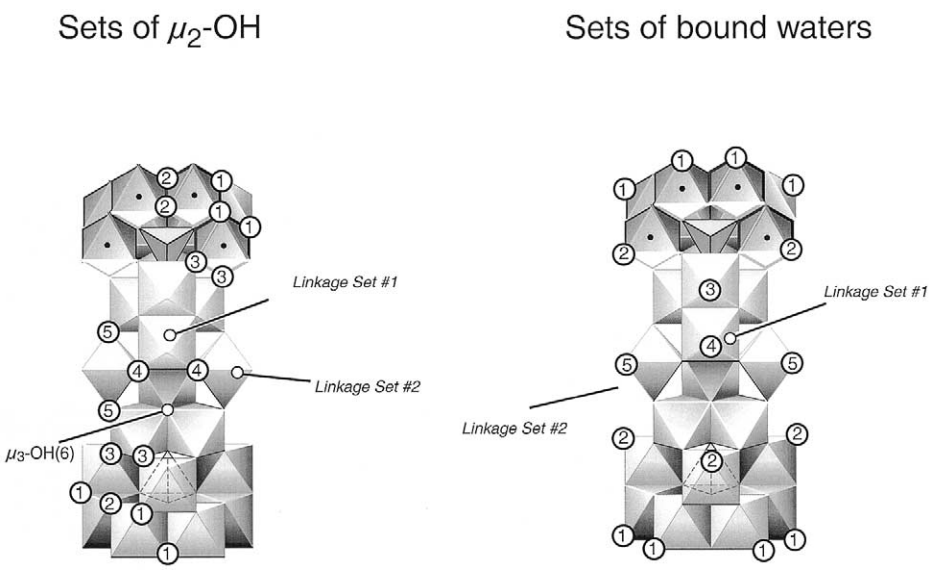

Fig. 3. Sets of topologically distinct μ_2-OH (left) and η-OH_2 (right) discussed in the text. The two sets of equatorial $Al(O)_6$ linkages are also identified, as in Figure 2.

4. Four μ_2-OH(4) that link corner-shared $Al(O)_6$ in the equatorial region of the Al_{30}, which lie between Linkage Sets #1 and #2 (Fig. 3), and are *cis* to two μ_3-OH.
5. Four μ_2-OH(5) linking corner-shared $Al(O)_6$ in the rotated trimeric (Al_3O_{13}) and Linkage Set #2 (Fig. 3) that are also *cis* to two μ_3-OH.
6. Six μ_3-OH(6) within the tetrameric cap formed by connecting Linkage Set #1 to the rotated trimeric group.

The μ_4-O sites in the Al_{30} (eight total) are very similar to those in the δ-Al_{13} molecules and link the two tetrahedrally coordinated aluminums ($Al(O)_4$) to the outer part of the molecule. These μ_4-O comprise two distinct sets based upon their positions relative to the rotated trimer.

There are 24 bound water molecules (η-OH_2) on the Al_{30} that comprise eight distinct sites in C_{2h} and can be grouped into five topological sets (Fig. 3):

1. Twelve η-OH_2 that are on the basal rings of the δ-Al_{13}-like moieties.
2. The remaining six η-OH_2 on the δ-Al_{13}-like moieties that are adjacent to the rotated (Al_3O_{13}) trimeric group.
3. Two η-OH_2 in the tetrameric caps that are *trans* to a μ_4-O.
4. Two η-OH_2 in the tetrameric caps that are on Linkage Set #1 of $Al(O)_6$.
5. Four η-OH_2 on Linkage Set #2 in the equatorial region.

These groupings are convenient for discussion of the NMR results below, which cannot resolve all of the distinct oxygen sites. We note that Allouche et al., (2001) found evidence that the Al_{30} sulfate salt exhibits C_c symmetry, which would require all 88 oxygens be inequivalent. For the Al_{30} aqueous complex, we believe any distortion from the topochemical symmetry is likely to be averaged to C_{2h} on the NMR time scales.

A qualitative guide to the reactivity of different oxygens in

Table 1. Structurally distinct oxygen sites on the Al_{30} complex.

OH-site[a]	type	polyhedral linkage	total	symmetrically distinct[b]
1	μ_2-OH	edge	18	4; 4:8:2:4
2	μ_2-OH	edge	12	4; 2:4:2:4
3	μ_2-OH	corner	12	3; 4:4:4
4	μ_2-OH	corner	4	1
5	μ_2-OH	corner	4	1
6	μ_3-OH	3-edges	6	2; 4:2

η-OH_2 site[a]	adjacent OH-sites	total	symmetrically distinct[b]
1	1,1,2,2	12	3; 4:4:4
2	1,1,3,3	6	2; 4:2
3	3,3,6,6	2	1
4	4,4,6,6	2	1
5	4,5,5	4	1

[a] Label numbers refer to Figure 3.
[b] Assuming C_{2h} symmetry. These numbers list the number of types of sites in the set (e.g., '4'), followed by the multiplicity of each (e.g., 4:8:2:4). When added, the number of positions sums to the total (e.g., 18).

Table 2. Solution compositions. The composition of sample 36_53 was measured by wet-chemical analysis and the solute concentrations in other samples, except pH, were calculated from the mass of salts and the volume of H_2 ^{17}O added. The total dissolved concentrations are in molar units. Precisions (triplicate analyses) for measurements are given in parentheses. n. d. = not detected; d. l. = at or below detection limit.

Sample	pH[1]	ΣAl	ΣNa	ΣSe	ΣMn	ΣCl	ΣBa
			Stock Solution				
36_53	4.67	0.997	$4.3 \cdot 10^{-3}$	$2.2 \cdot 10^{-6}$	...	0.574	0.0455
	(±0.039)	($\pm 1.6 \cdot 10^{-3}$)	(±0.003)	($\pm 1.1 \cdot 10^{-6}$)	...	(±0.026)	(±0.026)
			^{17}O-injection samples				
35_18	4.69	0.499	$2.15 \cdot 10^{-3}$	d. l.	0.2498	0.787	0.0228
35_21	4.61			as 35_18			
35_24	4.64			" "			
35_27	4.70			" "			
35_29[2]				" "			
			^{17}O-equilibrated sample				
35_42[2]		0.095	0.215		0.296	0.878	

[1] 25°C, electrode calibrated in 2.0 M NaCl [2] pH not measured; calculated concentrations

the Al_{30} can be found in studies of other aluminum multimers and inert-metal complexes (e.g., Springborg, 1988; Richens, 1997). Generally, lability decreases with the number of similar metals bonded to the oxygen. For example, at 25°C the characteristic time (τ_{298}) for exchange of the η-OH_2 in the Al_{13} multimer is $\tau_{298} \approx 1$ ms, for the two sets of μ_2-OH $\tau_{298} \approx 17$ h (μ_2-OH_{slow}) and $\tau_{298} \approx 1$ min (μ_2-OH_{fast}), yet the μ_4-O do not exchange with the solvent unless the Al_{13} molecules dissolve and then reassemble (Phillips et al., 2000).

2. METHODS

2.1. Composition of Experimental Solutions

The Al_{30} salt was prepared using a method similar to that described by Allouche et al. (2000) and its purity was determined by ^{27}Al-MAS NMR. Crystals of the Al_{30}-selenate salt were ground with $BaCl_2$ and extracted with ≈12 mL of isotopically normal water, followed by ultrasonic agitation and filtration. This extraction causes the crystals to dissolve and release Al_{30} molecules to solution, but the selenate is retained as a barium-selenate precipitate. The concentration of Al_{30} in the resulting stock solution (36_53) was 0.033(±10%) M and the aqueous Al_{30} complex accounts for virtually all of the dissolved aluminum. The analytical aluminum concentration in 36_53 was 0.997_1(±0.04)M and the analytical chloride concentration was 0.574_3(±0.0026) (Table 2). Assuming that all dissolved aluminum were present as Al_{30} complex, as indicated by the ^{27}Al-NMR spectra, the calculated cationic charge concentration is 0.598 mol/L, within 5% of the measured anionic concentration of the Cl^- counter ion (Table 2).

Oxygen-exchange rates were measured by an injection technique with ^{17}O-NMR detection. Injection experiments were begun by mixing 1.2 mL of ^{17}O-enriched water (35%, Isotec Laboratories) with 1.2 mL of the isotopically normal Al_{30} stock solution (sample 36_53), then acquiring ^{17}O NMR spectra as a function of time over several weeks. The initial ^{17}O-solution contained 0.5 mol/L $MnCl_2$ and the stock solution contained ≈0.033 mol/L in Al_{30} (Table 2). This procedure resulted in ≈0.017 mol/L solution of isotopically normal Al_{30} in a 0.25 mol/L solution of $MnCl_2$ at pH≈4.65±0.05 that was enriched to ≈17% in $H_2{}^{17}O$. before mixing, all of these solutions were separately brought into thermal equilibrium with a water bath at selected constant temperatures between 32 and 40°C. The time from mixing of the solutions to collection of the first spectrum was usually ≈7 min.

The pH is highly buffered by the Al_{30} and was nearly constant with time and temperature, so that pH measurements could be confidently completed after an experiment. The solution pH was determined using a combination electrode that was calibrated on the concentration scale by titrating solutions of 2.0 mol/L NaCl with a strong acid. The apparent ionic strength (I_a) of the experimental solution is extremely high (I_a>13 mol/L) because the +18 charge of the Al_{30} ion is squared in the equation for apparent ionic strength. Because of this high ionic strength, the uncertainty in the pH measurement arises from the junction-potential corrections and is probably on the order of ±0.2 units, which is much larger than the experimental precision of ±0.05 units.

The ^{17}O-equilibrated sample, 35_42, was prepared by adding 1.0 mL of 0.539 mol/L $AlCl_3$ to 4.0 mL 8% $H_2{}^{17}O$ and titrating with 0.110 mL of 10.0 mol/L NaOH solution at 75°C. The resulting solution had $\frac{\Sigma OH^-}{\Sigma Al} = 2.04$ and was aged for several weeks, with periodic examination via ^{27}Al-NMR, until the sample contained mostly Al_{30} as the dominant aluminum species.

3. RESULTS

3.1. Spectra of Isotopically Equilibrated Al_{30}

The ^{27}Al NMR spectrum of sample 35_42 (Fig. 4, top) indicates it contains the Al_{30} polyoxocation as the predominant aluminum-containing species, consistent with the bulk composition of the solution. The broad peak near +70 ppm arises from the central $Al(O)_4$ sites of Al_{30} (Rowsell and Nazar, 2000; Allouche et al., 2000) and corresponds to about 92% of the integrated intensity in the tetrahedral region. This sample also contains a small amount of Al_{13}, which yields the small, sharp peak near +63 ppm, and a polyoxocation of unknown structure that gives a shoulder near +76 ppm (the "Al_{P3}" of Fu et al., 1991). The absence of a peak near 0 ppm indicates very low concentration of monomeric aluminum species ($Al^{3+}(aq)$ + $AlOH^{2+}$... in rapid exchange equilibrium). The large peak near +10 ppm is the unresolved signal from all the octahedral aluminum in the polyoxocations.

The ^{17}O NMR spectra of the isotopically equilibrated sample (35_42) at 40°C (Fig. 5 -a) are broadly similar to those of other polyoxocations of aluminum (Thompson et al., 1987; Phillips et al., 2000; Casey et al., 2000; Casey and Phillips, 2001; Lee et al., 2002) and contain a sharp peak that we assign to bound water molecules near +22 ppm, a broader peak near +37 ppm and a narrow peak near +55 ppm. Signal from the solvent waters is broadened beyond detection by interaction with paramagnetic Mn(II) that was added to the solution before recording the NMR spectra. The appearance of this spectrum changes with temperature, primarily due to changes in peak widths. The peaks at +37 and +55 ppm narrow with increasing temperature, consistent with peak width dominated by quadrupolar relaxation, whereas the peak at +22 ppm broadens with in-

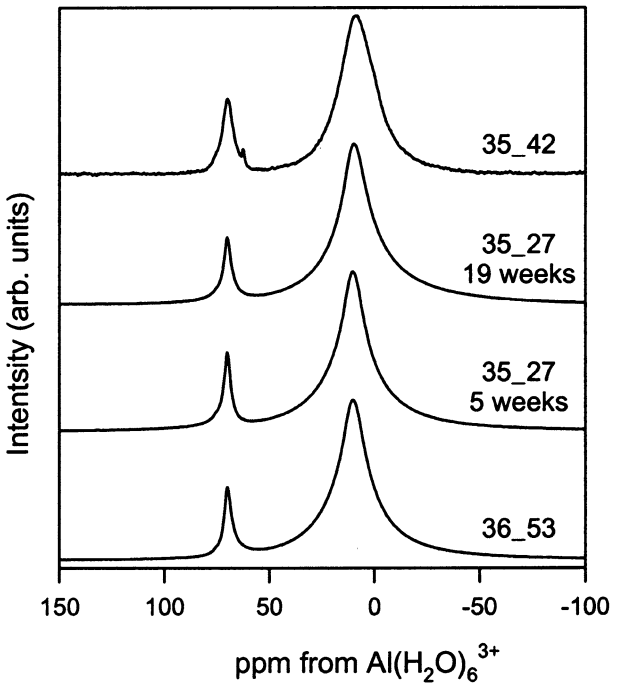

Fig. 4. ^{27}Al NMR spectra of Al_{30} samples used for this study, at 70°C. *Bottom:* 36_53 stock solution used as starting material for the oxygen isotopic equilibration experiments; *Middle (two spectra):* typical spectra during an oxygen exchange experiment, with elapsed time since addition of the ^{17}O-enriched Mn(II) solution. *Top:* 35_42 Al_{30} solution prepared in ^{17}O-enriched water. Peak at +70 ppm arises from the $Al(O)_4$ centers of the Al_{30} complex. Sample 35_42 contains a small amount of Al_{13} (δ = 63 ppm) and all samples contain a small amount of Al_{P3} impurity (δ = 76 ppm). Spectra acquired at 130.3 MHz with single-pulse excitation.

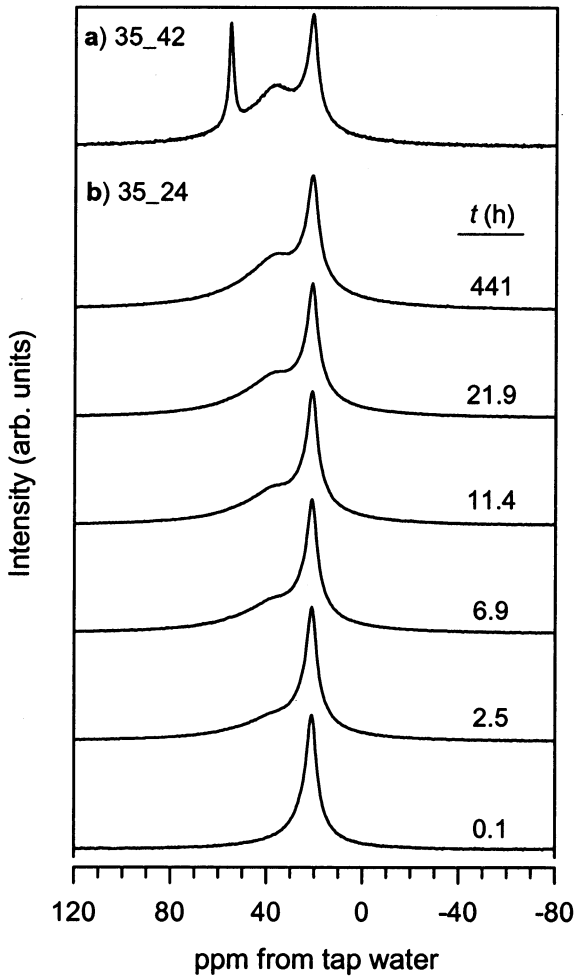

Fig. 5. ^{17}O NMR spectra at 40°C of Al_{30} samples; **a)** Sample 35_42, prepared with uniform ^{17}O-enrichment at all oxygen sites; **b)** Spectra from a typical oxygen isotope equilibration experiment (35_24, T = 313 K). Times are elapsed time since addition of ^{17}O-enriched water.

creasing temperature due to the influence of chemical exchange of these bound waters with solvent. Widths of the peaks at +37 and +22 ppm could not be quantified in any meaningful way because they comprise signals from many distinct sites and cannot be adequately fit by single Lorentzian-shaped curves (see Appendix 1).

The relative intensity (integrated area) of the peak at +22 ppm decreases significantly with increasing temperature over the interval 50–70°C as the exchange rate for distinct sets of bound waters become fast enough to broaden the corresponding resonance into the baseline. We were unable to measure the exchange rates of the bound waters with the line-broadening technique due to the unresolved contributions from the eight distinct sets of bound waters. However, the temperature range over which the signal could be observed suggests that the exchange rates for most of the bound waters are similar to those of the Al_{13} and $GaAl_{12}$ molecules (Phillips et al., 2000; Casey and Phillips, 2001).

Relative integrated intensities for the three peaks in the ^{17}O NMR spectrum of 35_42 were obtained from a least-squares fit to a sum of five Lorentzian curves. For an acceptable fit, the peaks at +37 and +22 ppm each required two curves, differing primarily in peak width, due to the large number of distinct sites (for C_{2h} symmetry, eight η-OH_2 and 15 μ-OH) on the Al_{30} complex (see Appendix 1). To compare the relative ^{17}O peak intensities to the stoichiometric ratios for Al_{30} we normalized the peak intensities such that the narrow, well-resolved peak at +55 ppm corresponds to the eight μ_4-O on the complex. The normalized intensities for the other peaks correspond to 56(±1) hydroxyls (+37 ppm) and 22(±1) bound waters (+22 ppm) at 40°C (estimated to 1σ uncertainties). These values indicate that all the Al_{30} hydroxyls are observed (56 by stoichiometry), but that about four of the 26 bound waters are not observed at these temperatures, most likely due to large peak width arising from very rapid exchange with the bulk waters. The concentrations of the other species (Al_{P3} and Al_{13}) are too low to significantly affect these intensity ratios. Any isotopic fractionation among the oxygens on the complex should be too small to detect by NMR, because solution 35_42 was prepared directly from ^{17}O-enriched water.

3.2. Rates of ^{17}O Isotopic Equilibration

The ^{27}Al NMR spectrum of the 36_53 (Fig. 4 bottom) shows the presence of Al_{30}, from the peak near +70 ppm that arises from its two unresolved $Al(O)_4$ sites, with a small amount of

the "Al_{P3}" species (corresponding to less than 5% of the $Al(O)_4$) that contributes a slight asymmetry to the tetrahedral Al peak that can be fitted by a peak centered near +76 ppm (Fu et al., 1991). No changes in the ^{27}Al-NMR spectra or pH were observed upon mixing with the ^{17}O-enriched Mn(II) solutions or over the subsequent course of any of the oxygen-exchange experiments (Fig. 4 middle), except for a constant downfield shift of peak positions in the Mn(II)-containing solutions. This shift arises from magnetic susceptibility effects and is corrected in Figure 4. Differences in peak widths between the 36_53 stock solution and sample 35_42 (Fig. 4 top and bottom) are due to differences in quadrupolar relaxation rates related to the much different ionic strengths of these solutions (Table 2).

The variations in the ^{17}O-NMR spectra with time after mixing the isotopically normal 36_53 solution with ^{17}O-enriched water (Fig. 5-b) are very similar to those observed for similar experiments with the MAl$_{12}$ ε-Keggin molecules (Phillips et al., 2000; Casey and Phillips, 2001; Lee et al., 2002). The first spectrum taken shortly after mixing (≈7 min) contains a large peak near +22 ppm, assigned to the bound water molecules (Fig. 5-b bottom). Compared with the signal from an external coaxial solution (peak near −100 ppm is not shown in Fig. 5), the intensity of the peak at +22 ppm shows no significant change as a function of time throughout the experiment, indicating that isotopic equilibration of the bound waters is very rapid.

At short times a shoulder is present downfield from the peak at +22 ppm that appears initially as an asymmetry near the baseline but gradually grows with time to a distinct peak centered near +37 ppm. We assign this peak at +37 ppm to the hydroxyl oxygens on the molecule, consistent with previous work on the MAl$_{12}$ ε-Keggin molecules (Phillips et al., 2000; Casey and Phillips, 2001; Lee et al., 2002). At all temperatures, the intensity ratio for the peak assigned to hydroxyls to that assigned to bound waters ($R(t) = I_{\delta=37ppm}/I_{\delta=22ppm}$) increases with time in several apparent steps (Fig. 6): an initial rapid increase to about $R(t) \approx 0.8$ over the course of several hours, followed by a slower rise to near $R(t) \approx 1.7$ over the first day, followed by a much slower, asymptotic approach to $R(t) \approx 2.4_5(\pm 0.1)$ over a period of 1–2 weeks.

These relative intensities were obtained from least-squares fits of the spectra as described above for sample 35_42, using two curves each for the peaks at +37 and +22 ppm. The fitted values are very sensitive to small phase adjustments (yielding variations of several percent), which results in uncertainties that are dominated by non-random errors and much greater than for earlier studies of the ε-Keggin MAl$_{12}$ complexes. For these experiments, $R(t)$ represents the average number of hydroxyls that have undergone exchange, normalized to the number of observed bound waters, because the intensity of the bound water peak does not change significantly with time and isotopic equilibration of the cluster does not significantly alter the isotopic composition of the reservoir.

After several weeks of equilibration, $R(t)$ approaches a value very similar to that obtained for sample 35_42 ($56(\pm 1)/22(\pm 1) = 2.5_5(\pm 0.1)$), which was prepared with uniform isotopic composition among the oxygen sites. None of the isotopic equilibration experiments produced a peak near +55 ppm for the μ_4-O groups (cf. Fig. 5-a and 5-b). Assuming our detection limit is about one percent of the integrated intensity, this result indicates that the characteristic time for steady-state exchange of the μ_4-O with solvent is greater than about 33 weeks.

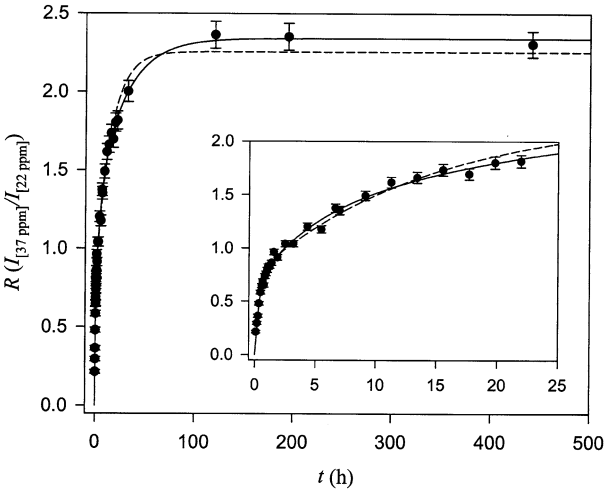

Fig. 6. Typical plot of the ratio of integrated intensity for the ^{17}O NMR peak at +37 ppm, assigned to hydroxyl sites, to that for the peak at +22 ppm due to bound water molecules with time elapsed since addition of ^{17}O-enriched water. Sample 35_24, T = 313 K. Line represents a weighted least squares fit of the data to Eqn. 1, yielding the coefficients and time constants in Table 3. Dashed line is a similar fit employing two time constants (cf. three for Eqn. 1), which yields low values of $R(t)$ at long times for all samples. Inset shows initial data at expanded scale.

For comparison of the results at different temperatures, we fit $R(t)$ to a sum of three exponentials:

$$R(t) = a_1(1 - \exp(\tau_1/t)) + a_2(1 - \exp(\tau_2/t)) + a_3(1 - \exp(\tau_3/t)) \quad (1)$$

using weighted non-linear least-squares methods, where the constants a_i are proportional to the number of sites in a stoichiometric unit contributing to the peak intensity, and τ_i are characteristic time constants (Table 3). Three time constants could describe the observed changes in $R(t)$ at all temperatures, even though the Al_{30} complex contains 15 inequivalent hydroxyl positions in at least six topologically distinct groups (Fig. 3, Table 1). Fits using two time constants modeled the data reasonably well at short times, but gave systematically low values for $R(t)$ at long reaction times for all samples (Fig. 6). Uncertainties in the fitted parameters listed in Table 3 are the square root of the corresponding diagonal elements of the final covariance matrix. These values resulted from weighting the $R(t)$ values according to an estimated uncertainty of ± 0.01 (1σ) in the absolute integrated intensities of the hydroxyl and bound water peaks, normalized to a total spectral intensity of unity, which yields increasing uncertainty in $R(t)$ with reaction time (Fig. 6). These uncertainties are given solely to illustrate minimum values, because the spectral data reduction and fitting are subject to systematic and non-random errors due to the limited resolution and sensitivity of fitted intensities to baseline and phase corrections.

The variability in the fitted values a_i and τ_i (Table 3) at similar conditions (e.g., 32°C) is too large for detailed interpretation. As a result, we do not attempt to derive activation

Table 3. Results of least-squares fits of integrated intensity ratios to Equation 1 for the isotopic-equilibration experiments.

Sample	T (K)	a_1 (±0.04)[d]	τ_1(h) (±0.1)	a_2 (±0.07)	τ_2(h)	a_3 (±0.10)	τ_3(h)	A[a] (±0.13)	⟨τ(h)⟩[b]	n_1[c] (±2)	n_2 (±3)	n_3 (±4)
35_18	305	0.42	0.3	0.73	3 (1)	1.29	54 (10)	2.44	29	10	17	30
35_21	309	0.78	0.6	0.82	16 (5)	0.88	80 (30)	2.48	34	18	19	20
35_24	313	0.67	0.3	0.59	5 (2)	1.10	28 (10)	2.36	14	16	14	26
35_27	305	0.56	0.3	0.51	3 (1)	1.33	43 (10)	2.41	24	13	12	31
35_29	305	0.69	0.5	0.67	6 (2)	1.20	89 (20)	2.56	43	15	15	26

[a] $A = a_1 + a_2 + a_3$; [b] Weighted average time constant: $\langle\tau\rangle = A^{-1}\sum_{i=1}^{3} a_i\tau_i$; [c] $n_i = 56 \cdot a_i \cdot A^{-1}$; [d] Minimum uncertainties (see text); those for τ_2 and τ_3 are given as last digits.

energies from changes in equilibration times with this small range in experimentally accessible temperatures. However, there is some broad agreement with respect to the numbers of exchanging hydroxyls in each apparent step and the approximate corresponding timescales. Excluding sample 35_21, which produced unusually large scatter in the kinetic curve, the most labile group consists of about 14(±3) of the hydroxyls, a similar number, 14(±3), have intermediate reactivity, whereas a significantly larger number of the hydroxyls (28(±4)) are comparatively inert (Table 3). These values assume that all 56 hydroxyls exchange, as is suggested by comparison of the final *R(t)* values attained at isotopic equilibrium (equal to the fitted *A* values, Table 3) with the results for sample 35_42.

4. DISCUSSION

4.1. Comparison with other Aluminum Complexes

The structural complexity of the Al_{30} molecule precludes evaluation of the full rate law for exchange reactions of each individual oxygen site. Furthermore, it is difficult to substantially lower pH for long periods of time without dissociating some of the Al_{30} molecule into smaller multimers of unknown stoichiometry and lifetimes, and raising pH causes gel to form. However, even these partial results provide important conclusions that relate to the reactivity of mineral/fluid interfaces.

First, it is clear that the rates of isotopic equilibration of oxygens in hydroxyl bridges fall within the range observed for other aluminum complexes, which suggests a strategy for assigning the kinetic results to groups of structural sites. Values of τ_2 (Table 3) range from 3 to 6 h in this temperature range (ignoring sample 35_21), compared to 2.5 to 7 h measured for the μ_2-OH_{fast} of $GaAl_{12}$ (at 40 and 32°C, respectively; Casey and Phillips, 2001). Similarly, τ_3 ranges from about 30 to 90 h for Al_{30}, compared to 47 to 169 h for μ_2-OH_{slow} of $GaAl_{12}$ (40–32°C). In comparison, the hydroxyls of Al_{13} appear to be anomalously labile (e.g., lifetime less than one minute for μ_2-OH_{fast} at 32°C; Casey et al., 2000), which might relate to the strain caused by the unusually long bonds between the Al(4) and the μ_4-O (see Table 4 in Lee et al., 2002).

Comparison of the fitted n_i values (Table 3) to the stoichiometric ratios (Table 1) suggests that the least-labile group of Al_{30} hydroxyls probably includes the μ_2-OH(1)-type sites (see above), because there are more of these (18) than would be consistent with fitted values of n_1 or n_2. Considering the structural similarity of these μ_2-OH(1) sites to the μ_2-OH^b of the ε-Keggin MAl_{12} molecules (cf. Fig. 1 and 3) and the similar timescale of reaction of μ_2-OH(1) sites (represented by τ_3) and μ_2-OH_{slow} of $GaAl_{12}$, these observations suggest assignment of the μ_2-OH_{slow} site to the structural site μ_2-OH^b (Fig. 1) in the $GaAl_{12}$ molecules; that is, the μ_2-OH_{slow} is within a trimeric group in the $GaAl_{12}$, not between trimers, which makes intuitive sense. Likewise, assignment of the μ_2-OH(2) site in the Al_{30} to the group of intermediate lability is suggested by its structural and kinetic similarity to the μ_2-OH^a and μ_2-OH_{fast} of $GaAl_{12}$, respectively, and is consistent with the stoichiometric ratios and fitted n_2 values. The presence of a group of about 10 to 16 very labile hydroxyls (τ_1 of about 0.5 h) distinguishes the present results for the Al_{30} from those for the $GaAl_{12}$. These highly reactive sites probably correspond to hydroxyls in corner-linked configurations (e.g., μ_2-OH(3)), because there are no analogous sites on the $GaAl_{12}$. To account for the large n_3 values requires that some of the remaining sites (one or more of μ_2-OH(4); μ_2-OH(5); μ_3-OH(6)) belong to the more slowly reacting group of hydroxyl sites. We speculate that the μ_3-OH are probably less labile, considering that three bonds must be broken to exchange this oxygen with solvent water. The total number of μ_2-OH(1) and μ_3-OH(6) hydroxyls per molecule (18 + 6) approaches the fitted n_3 values.

Secondly, the μ_3-OH sites are observed to exchange with the aqueous solution, which is important because minerals such as boehmite expose highly coordinated oxygens to the aqueous phase. We expect the μ_2-OH and μ_3-OH bridges near edge and kink sites at mineral surfaces to exchange with water molecules in bulk solution on a similar time scale. Using 100 kJ/mol as a typical apparent activation energy for exchange of a hydroxyl bridge (Springborg, 1988; Phillips et al., 2000; Casey and Phillips, 2001), rates of exchange should proceed $\approx 10^2$ times more slowly at field temperatures of ≈5°C than at the experimental temperatures of 40°C. Extrapolation of these results suggests that μ_2-OH groups at the surface edges of aluminum (hydr)oxide minerals will isotopically exchange with bulk solution within a period of months at 5°C.

Thirdly, most of the bound water molecules on the Al_{30} appear to equilibrate with bulk solution at rates that are similar to those observed for other aluminum complexes. Although signal cannot be resolved for individual η-OH_2 sites on the Al_{30}, the composite ^{17}O-NMR line width and the observation that this peak becomes broader with increased temperature suggests that the rates of exchange on the Al_{30} fall into a similar range as for aluminum monomers and MAl_{12} ε-Keggin

species ($\tau_{ex}^{298} \approx 0.01 - 0.0001$ s; Casey and Phillips, 2001 and references therein). This result is consistent with our previous work indicating a limited range for rates of exchange of η-OH_2 sites from aluminum complexes and supports our earlier speculation that rates of exchange of η-OH_2 from the surfaces of fully protonated aluminum (hydr)oxide minerals will fall into a similar range as well.

Fourthly, four of the 26 bound waters react much faster than the others. We speculate that these highly reactive waters probably correspond to the set of four η-OH_2 that are *cis* to two μ_3-OH in the tetrameric cap of the δ-Al_{13}-like moieties (Fig. 2) in the Al_{30} molecule, which are formally overbonded. Based on stoichiometry, they could also correspond to the four η-OH_2 associated with Linkage Set #2, which are *cis* to three μ_2-OH and or *trans* to another. In other multimers (see Crimp et al., 1994) rates of exchange of bound and bulk water molecules increases with the number of inner-sphere hydroxyls.

These measurements are part of a series of experiments that are intended to provide results for computational simulation. The rate data presented in this study correspond to composites of elementary or near-elementary reactions. It is our hope that, by coupling simulation and experiment, we can evaluate our ability to simulate reactions that affect oxygens in these molecules and then for hydrated mineral surfaces. In considering this point one need remember that the proton charge densities on these clusters fall in the same range as protonated aluminum (hydr)oxide minerals. These aqueous complexes also create considerable electrostatic fields and solvent-ordering effects in the aqueous solution that are similar to those associated with charged mineral surfaces. The Al_{30} molecules in a 0.033 mol/L solution each have a +18 charge and are separated from one another only by an average of about 12 bulk water molecules.

Acknowledgments—The authors are grateful to three anonymous referees and David Wesolowski for providing particularly insightful criticisms of the text that clarified our message. Support for this research was from the U.S. NSF via grant EAR 0101246 and from the U.S. DOE DE-FG03–96ER14629. The NMR spectrometers were purchased using grants from the National Institute of Health (NIH 1S10-RR04795) and the National Science Foundation (NSF BBS88–094739) and we also acknowledge the Keck Foundation for support of the solid-state NMR center at U.C. Davis.

Associate editor: D. J. Wesoloski

REFERENCES

Allouche L., Gérardin C., Loiseau T., Férey G., and Taulelle F. (2000) Al_{30}: A giant aluminum polycation. *Angew. Chem. Int. Ed.* **39,** 511–514.

Allouche L., Huguenard C., and Taulelle F. (2001) 3QMAS of three aluminum polycations: space group consistency between NMR and XRD. *J. Phys. Chem. Solids* **62,** 1525–1531.

Bradley S. M., Kydd R. A., and How R. F. (1993) The structure of Al gels formed through the base hydrolysis of Al^{3+} aqueous solutions. *J. Coll. Interface Sci.* **159,** 405–412.

Casey W. H., Phillips B. L., Karlsson M., Nordin S., Nordin J. P., Sullivan D. J., and Neugebauer-Crawford S. (2000) Rates and mechanisms of oxygen exchanges between sites in the $AlO_4Al_{12}(OH)_{24}(H_2O)_{12}{}^{7+}$(aq) complex and water: Implications for mineral surface chemistry. *Geochim. Cosmochim. Acta* **64,** 2951–2964.

Casey W. H. and Phillips B. L. (2001) The kinetics of oxygen exchange between sites in the $GaO_4Al_{12}(OH)_{24}(H_2O)_{12}{}^{7+}$(aq) molecule and aqueous solution. *Geochim. Cosmochim. Acta* **65,** 705–714.

Crimp S. J., Spiccia L., Krouse H. R., and Swaddle T. W. (1994) Early stages of the hydrolysis of chromium(III) in aqueous solutions. 9. Kinetics of water exchange on the hydrolytic dimer. *Inorg. Chem.* **33,** 465–470.

Fu G., Nazar L. F., and Bain A. D. (1991) Aging processes of alumina sol-gels: characterization of new aluminum polyoxocations by ^{27}Al-NMR spectroscopy. *Chem. Mater.* **3,** 602–610.

Hunter D. and Ross D. S. (1991) Evidence for a phytotoxic hydroxy-aluminum polymer in organic soil horizons. *Science* **251,** 1056–1058.

Lee A. P., Phillips B. L., and Casey W. H. (2002) The kinetics of oxygen exchange between the $GeO_4Al_{12}(OH)_{24}(OH_2)_{12}{}^{8+}$(aq) molecule and aqueous solutions. *Geochim. Cosmochim. Acta* **66,** 577–587.

Phillips B. L., Casey W. H., and Karlsson M. (2000) Bonding and reactivity at oxide mineral surfaces from model aqueous complexes. *Nature* **404,** 379–382.

Pope M. T. (1983) *Heteropoly and isopoly oxometalates*, 165 p. Springer-Verlag, New York.

Rao G. V. and Rao K. S. J. (1992) Evidence for a hydroxy-aluminum polymer (Al_{13}) in synaptosomes. *FEBS Lett.* **311,** 49–50.

Richens D. T. (1997) The Chemistry of Aqua Ions. Wiley, 592 pp.

Rowsell J. and Nazar L. F. (2000) Speciation and thermal transformation in alumina sols: structures of the polyhydroxyoxoaluminum cluster $(Al_{30}O_8(OH)_{56}(H_2O)_{26})^{18+}$ and its Keggin moieté. *J. Am. Chem. Soc.* **122,** 3777–3778.

Springborg J. (1988) Hydroxo-bridged complexes of chromium(III), cobalt(III), rhodium(III) and iridium(III). *Adv. Inorg. Chem.* **32,** 55–169.

Thompson A. R., Kunwar A. C., Gutowsky H. S., and Oldfield E. (1987) Oxygen-17 and aluminum-27 nuclear magnetic resonance spectroscopic investigations of aluminum(III) hydrolysis products. *J. Chem. Soc. Dalton Trans.* **1987,** 2317–2322.

Yu P., Phillips B. L., and Casey W. H. (2001) Water exchange in fluoroaluminate complexes in aqueous solution: A variable temperature multinuclear NMR study. *Inorg. Chem.* **40,** 4750–4754.

Wehrli B., Wieland E., and Furrer G. (1990) Chemical mechanisms in the dissolution kinetics of minerals-the aspect of active sites. *Aqua. Sci.* **52,** 3–31.

APPENDIX

The relative integrated intensities of the ^{17}O NMR peaks at +37 and +22 ppm for the oxygen isotopic equilibration experiments and for the uniformly ^{17}O-enriched sample 35_42 were determined by non-linear least-squares fits of the spectra to a sum of Lorentzian-shaped curves (Fig. A1). In all cases, fits employing one curve for each of these peaks

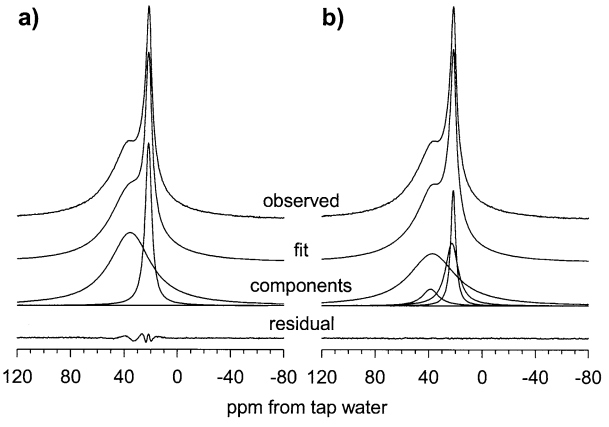

yield residuals that are significantly larger than spectral noise, and that display low-frequency oscillations indicating a poor model for the data (Fig. A1a). This result is not surprising considering that the Al_{30} molecule contains fifteen inequivalent hydroxyl positions and eight inequivalent bound waters, all of which might exhibit different peak

widths and positions. Lorentzian-shaped curves are appropriate for the Fourier-transform of exponentially decaying signals in the time domain. Use of Voigt curves (convolution of Lorentzian and Gaussian functions) did not significantly improve the fit.

We found that the model shown in Figure A1b produced much better fits to the observed spectra under all conditions studied, with a minimum number of additional components. Addition of two curves, one near +37 and another near +22 ppm, with differing peak widths, reduced χ^2 by a factor of about three. However, formal statistical tests are not strictly valid because errors are not be distributed normally due to the subjective nature of baseline and phase corrections. The physical basis for this model is the observation in previous studies (see Casey and Phillips, 2001 and references therein) that the peak positions for μ_2-OH and bound waters exhibit little variation among aqueous Al-complexes but that peak widths vary with the nuclear quadrupolar coupling constant and, for η-OH_2, the rate of chemical exchange with solvent. For the isotopic equilibration experiments at long reaction times, the initial guess was similar to that shown in Figure A1b and all parameters (area, width, and position) for each curve were allowed to vary during minimization of χ^2. The principal change among fits to spectra obtained at different reaction times was in the height of the broader, more intense peak at +37 ppm. At short reaction times only a single peak at +37 ppm was used, due to the low intensity of signal in this region. The cross-over to a four-component fit was made at an intermediate reaction time for which the three-component and four-component fits gave a similar ratio for the sums of integrated intensities for curves centered near +37 vs. those at +22 ppm. These models were used only to determine the relative areas of the peaks near +37 and +22 ppm; no additional physical significance is implied. For fits to sample 35_42, a fifth curve was added, near +55 ppm, to account for signal from the μ_4-O (cf. Fig. 5a).